

Quantum memory for images – a quantum hologram

Denis V. Vasilyev¹, Ivan V. Sokolov^{1,*}, and Eugene S. Polzik^{2,3,†}

¹ V. A. Fock Physics Institute, St. Petersburg University, 198504 Petrodvorets, St. Petersburg, Russia

² QUANTOP, Danish Research Foundation Center for Quantum Optics, DK 2100 Copenhagen, Denmark, and

³ Niels Bohr Institute, DK 2100 Copenhagen, Denmark

Matter-light quantum interface and quantum memory for light are important ingredients of quantum information protocols, such as quantum networks, distributed quantum computation, etc [1]. In this Letter we present a spatially multimode scheme for quantum memory for light, which we call a *quantum hologram*. Our approach uses a multi-atom ensemble which has been shown to be efficient for a single spatial mode quantum memory. Due to the multi-atom nature of the ensemble it is capable of storing many spatial modes, a feature critical for the present proposal. A quantum hologram has a higher storage capacity compared to a classical hologram, and is capable of storing quantum features of an image, such as multimode superposition and entangled quantum states, something that a standard hologram is unable to achieve. Due to optical parallelism, the information capacity of the quantum hologram will obviously exceed that of a single-mode scheme.

PACS numbers: 03.67.Mn, 32.80.Qk

One of the challenges in the field of quantum information is the development of a quantum interface between light and matter. At the quantum interface quantum states are either transferred between light and matter (quantum memory) or/and an entangled matter-light state is generated, which, e.g., is the basis for quantum teleportation. The quantum memory for light allows for the high fidelity exchange (transfer, storage and readout) of quantum states between light and long-lived matter degrees of freedom. Such interfaces will be an essential component of long distance quantum communication (quantum repeaters) and quantum computing networks. Various approaches to the quantum interface with atomic ensembles have been developed recently, including the quantum-nondemolition (QND) interaction (for reviews see [2] and [3]), electromagnetically induced transparency [4], and Raman processes [5, 6]. The present multi-mode proposal is based on the QND-type interaction which has been recently used for high-fidelity quantum memory [7] and teleportation [8] of a single-mode light. Up to now the work on light-atoms interface has been limited to the case of a single spatial mode of light and a single spatial mode of atomic ensembles.

On the other hand, multimode parallel quantum protocols for light only, such as quantum holographic teleportation [9, 10] and quantum dense coding of optical images [11] have been elaborated recently. The protocols of quantum imaging are based on the use of broadband spatially multimode light beams in an entangled Einstein - Podolsky - Rosen (EPR) quantum state.

In this Letter we develop theoretically a multimode parallel quantum memory for light, where an input signal is carried by a distributed in space and time wavefront (an optical image). Atomic ensembles used so far only for a single mode storage are inherently suitable for quantum holograms due to the possibility for storage of many spatial modes, which markedly distinguishes them

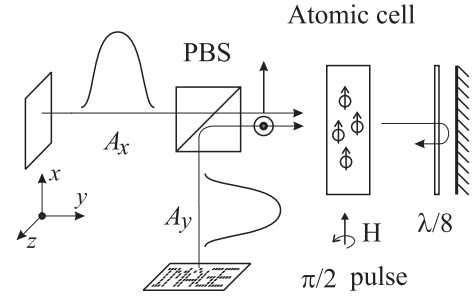


FIG. 1: The scheme of the write stage of the quantum hologram

from a single atom memory.

We utilize the two-pass storage and readout protocols previously proposed for a single mode scenario [2]. Multimode generalization for other single mode memory protocols, such as QND interaction followed by a quantum feedback onto atoms [7], and multi-pass protocols [12, 13] will be discussed elsewhere.

The key parameter for a quantum hologram is a spatial element (pixel). We use squeezed light to enhance the fidelity of the readout of the hologram, therefore in the following we investigate the relation between the pixel size and the transverse coherence length of squeezing. We conclude with calculations of the overall fidelity per pixel for the full cycle of the holographic memory.

The scheme, illustrating the write stage of our quantum memory protocol is shown in Fig. 1.

Consider an ensemble of atoms fixed at random positions with a spin $\frac{1}{2}$ both in the ground and in the excited state. The long-lived ground state spin of an atom \vec{J}^a is initially oriented in the vertical direction x . A classical off-resonant x -polarized plane wave of frequency ω_0 with a slowly varying amplitude A_x (taken as real) propagates in the z -direction. An input signal is represented by a

weak quantized y -polarized field of the same frequency and average direction of propagation with an amplitude $A_y(\vec{r}, t) \ll A_x$. In what follows we consider this multimode input field in the paraxial approximation. The QND light-matter interaction leads to two basic effects: (i) the Faraday rotation of light polarization due to longitudinal z -component of collective atomic spin; and (ii) the atomic spin rotation, caused by unequal light shifts of the ground state sub-levels with $m_z = \pm 1/2$ in the presence of circular light polarization. The relevant part of the Hamiltonian is [3]:

$$H = \frac{2\pi k_0 |d|^2}{\omega_{eg} - \omega_0} \int_V d\vec{r} \sum_a J_z^a S_z(\vec{r}, t) \delta(\vec{r} - \vec{r}_a). \quad (1)$$

Here ω_{eg} is the frequency of the atomic transition, d is the dipole matrix element, and $k_0 = \omega_0 c$. The z -component of the Stokes vector is $S_z(\vec{r}, t) = -iA_x(A_y(\vec{r}, t) - A_y^\dagger(\vec{r}, t))$. The amplitude A_y is defined via

$$A_y(z, \vec{\rho}, t) = \int \frac{dk_z}{2\pi} \int \frac{d\vec{q}}{(2\pi)^2} \sqrt{\frac{\omega(k)}{k_0}} a_y(\vec{k}) \times \exp[i(\vec{q} \cdot \vec{\rho} + (k_z - k_0)z - (\omega(k) - \omega_0)t)], \quad (2)$$

here $a_y(\vec{k})$ and $a_y^\dagger(\vec{k})$ – the annihilation and creation operators for the wave \vec{k} , which obey standard commutation relations $[a_y(\vec{k}), a_y^\dagger(\vec{k}')] = (2\pi)^3 \delta(\vec{k} - \vec{k}')$, $[a_y(\vec{k}), a_y(\vec{k}')] = 0$. In the paraxial approximation we have $[A_y(z, \vec{\rho}, t), A_y^\dagger(z, \vec{\rho}', t')] = \delta(t - t') \delta(\vec{\rho} - \vec{\rho}')$, where $\vec{r} = (\vec{\rho}, z)$, $\vec{k} = (\vec{q}, k_z)$. The space-dependent canonical variables for the input light are defined as quantities averaged over the interaction time T :

$$X_L(\vec{\rho}) = \frac{1}{\sqrt{T}} \int_T dt \frac{A_y(0, \vec{\rho}, t) + A_y^\dagger(0, \vec{\rho}, t)}{\sqrt{2}}, \quad P_L(\vec{\rho}) = \frac{1}{\sqrt{T}} \int_T dt \frac{A_y(0, \vec{\rho}, t) - A_y^\dagger(0, \vec{\rho}, t)}{i\sqrt{2}}, \quad (3)$$

and obey the commutation relations

$$[X_L(\vec{\rho}), P_L(\vec{\rho}')] = i\delta(\vec{\rho} - \vec{\rho}'). \quad (4)$$

In this Letter we will neglect the diffraction over the length L of the atomic layer, thus assuming that the Rayleigh length associated with the pixel linear size \sqrt{S} is much larger than L , i. e. $S \gg L\lambda$. A more general theory for quantum holograms, including the effects of diffraction and spatial density fluctuations of atoms will be presented in a forthcoming publication [16]. For a thin atomic layer located at $z = 0$, we introduce the surface density of the collective spin $\vec{J}(\vec{\rho}) = \sum_a \vec{J}_a \delta(\vec{\rho} - \vec{\rho}_a)$. The averaged over random positions of atoms commutation relation for y, z components of the collective spin is

$$[\overline{J_y(\vec{\rho})}, \overline{J_z(\vec{\rho}')}] = i \sum_a \langle J_x^a \rangle \overline{\delta(\vec{\rho} - \vec{\rho}_a) \delta(\vec{\rho}' - \vec{\rho}_a)}^a =$$

$$in_a \langle J_x^a \rangle \delta(\vec{\rho} - \vec{\rho}'). \quad (5)$$

Here n_a is the average surface density of atoms. The canonical variables for the spin subsystem

$$X_A(\vec{\rho}) = \frac{J_y(\vec{\rho})}{\sqrt{n_a \langle J_x^a \rangle}}, \quad P_A(\vec{\rho}) = \frac{J_z(\vec{\rho})}{\sqrt{n_a \langle J_x^a \rangle}}, \quad (6)$$

obey the canonical commutation relations analogous to (4).

In what follows both the write and readout procedures are performed in three steps. The input, two intermediate, and output variables are labelled by the (in), (1), (2), and (out) superscripts. The label W (R) indicates the write (readout) stages of the overall protocol. The transformation of atomic and field variables in the first passage of the signal looks similar to that described in [2, 7]:

$$\begin{aligned} X_L^{W(1)}(\vec{\rho}) &= X_L^{W(in)}(\vec{\rho}) + \kappa P_A^{W(in)}(\vec{\rho}), \\ P_L^{W(1)}(\vec{\rho}) &= P_L^{W(in)}(\vec{\rho}), \\ X_A^{W(1)}(\vec{\rho}) &= X_A^{W(in)}(\vec{\rho}) + \kappa P_L^{W(in)}(\vec{\rho}) \left(1 + \frac{\delta J_x^a(\vec{\rho})}{n_a \langle J_x^a \rangle}\right), \\ P_A^{W(1)}(\vec{\rho}) &= P_A^{W(in)}(\vec{\rho}). \end{aligned} \quad (7)$$

Here the coupling constant $\kappa = \alpha_0 \eta = 1$, where α_0 is the resonant optical depth and η is the probability of spontaneous emission [3]. Since $\eta \ll 1$ is required in order to neglect spontaneous emission, the usual condition $\alpha_0 = \lambda^2 n_a / 2\pi \gg 1$ should be fulfilled.

A non-trivial last term in the 3rd equation arises due to spatial fluctuations of the atomic density. It accounts for the fact, that the local value of the rotated collective spin and the local value of the coupling constant may differ from the average value. The effect of this term depends on the size of an elementary pixel. Under the conditions $\lambda^2 n_a / 2\pi \gg 1$ and $S \gg L\lambda$, where $L \gg \lambda$, the number of atoms per pixel is large, and we can neglect the influence of the atomic density fluctuations.

At the second step, the atomic spins are rotated around the x -axis by the $\pi/2$ pulse of an auxiliary magnetic field. The similar rotation of the Stokes vector of light is performed by the reflection of the signal wave from a mirror and by the double passage through $\lambda/8$ plate. This is described by the transformation $X_A^{W(2)} = -P_A^{W(1)}$, $P_A^{W(2)} = X_A^{W(1)}$, $X_L^{W(2)} = -P_L^{W(1)}$, $P_L^{W(2)} = X_L^{W(1)}$.

At the third step, the signal wave again propagates through the atoms. The transformation “(2) \rightarrow (out)” of the light and matter variables is the same as at the “(in) \rightarrow (1)” step, see (7). After all three steps of the write procedure, we arrive at

$$\begin{aligned} X_L^{W(out)}(\vec{\rho}) &= X_A^{W(in)}(\vec{\rho}), \\ P_L^{W(out)}(\vec{\rho}) &= P_A^{W(in)}(\vec{\rho}) + X_L^{W(in)}(\vec{\rho}), \end{aligned}$$

$$\begin{aligned} X_A^{W(out)}(\vec{\rho}) &= X_L^{W(in)}(\vec{\rho}), \\ P_A^{W(out)}(\vec{\rho}) &= P_L^{W(in)}(\vec{\rho}) + X_A^{W(in)}(\vec{\rho}). \end{aligned} \quad (8)$$

As seen from (8), the write procedure transfers the input signal variables onto the collective atomic spin. One can achieve a perfect light-matter state transfer provided the initial fluctuations $X_A^{W(in)}(\vec{\rho})$ of the collective spin are suppressed (squeezed) with a sufficient spatial resolution. Spin squeezing for a spatially single-mode configuration was demonstrated in [14, 15]. An extension to a multi-mode case will be analyzed elsewhere [16].

Note that after the first pass (7) only one quadrature of light is written onto the hologram. For a classical hologram this leads to a well known effect when the readout produces two images: the real and the imaginary one.

The transformation (8) describes the state exchange between light and matter. The same 3-step procedure can be used to transfer the quantum state of atoms created at the write stage onto the readout light wave. By substituting in (8) the label W to R, we obtain the transformation for the readout part of the protocol. The same reasoning as above suggests that for the high fidelity readout one needs to use the spatially multimode squeezed light with suppressed fluctuations $X_L^{R(in)}(\vec{\rho})$.

The ultimate goal of the protocol is to transfer a quantum state of the input (at the write stage) light signal to the output (at the readout stage) light. By combining the described above transformations, we can relate the input and output variables of the total write + readout protocol of quantum hologram:

$$\begin{aligned} X_L^{R(out)}(\vec{\rho}) &= X_L^{W(in)}(\vec{\rho}) + F_X(\vec{\rho}), \\ P_L^{R(out)}(\vec{\rho}) &= P_L^{W(in)}(\vec{\rho}) + F_P(\vec{\rho}). \end{aligned} \quad (9)$$

This transformation is analogous to the one describing quantum holographic teleportation of an optical image [9, 10]. The noise contributions specific for our model of memory are given by

$$F_X(\vec{\rho}) = 0, \quad F_P(\vec{\rho}) = X_A^{W(in)}(\vec{\rho}) + X_L^{R(in)}(\vec{\rho}). \quad (10)$$

Consider the field amplitude averaged over the surface S_i of a square pixel i of area S . The averaged noise amplitudes and the covariance matrix are

$$F_{X,P}(i) = \frac{1}{\sqrt{S}} \int_{S_i} d\vec{\rho} F_{X,P}(\vec{\rho}), \quad (11)$$

$C^X(i, j) = \langle F_X(i) F_X(j) \rangle$, $C^P(i, j) = \langle F_P(i) F_P(j) \rangle$. Assume the input signal field to be in the spatially multimode coherent state. The fidelity for an array of N pixels is related [10] to the covariance matrix as

$$F_N = [\det(\delta_{ij} + C^X(i, j)) \det(\delta_{ij} + C^P(i, j))]^{-1/2}. \quad (12)$$

We evaluate the fidelity for two initial states of the collective spin subsystem: (i) the coherent spin state with atomic spins oriented in the vertical x -direction with the fluctuations $X_A^{W(in)}(\vec{\rho}) = X_A^{(vac)}(\vec{\rho})$, $P_A^{W(in)}(\vec{\rho}) = P_A^{(vac)}(\vec{\rho})$, and (ii) the perfect spin squeezed state with the same average orientation, when $X_A^{W(in)}(\vec{\rho}) = X_A^{(sq)}(\vec{\rho}) \rightarrow 0$.

The vacuum state quadrature amplitudes, averaged over the pixel, have the variance $\langle X_A^{(vac)}(i) X_A^{(vac)}(j) \rangle = \delta_{i,j}/2$, and similar for $P_A^{(vac)}(i)$.

The state of the input light wave used for the readout of the quantum memory is a spatially multimode squeezed state, $X_L^{R(in)}(\vec{\rho}) = X_L^{(sq)}(\vec{\rho})$, $P_L^{R(in)}(\vec{\rho}) = P_L^{(sq)}(\vec{\rho})$.

The spatially multimode squeezed light can be generated in a nonlinear crystal with $\chi^{(2)}$ nonlinearity. For definiteness we assume the collinear degenerate wave matching in the crystal. The increase of fidelity is achieved by the suppression (squeezing) of the quadrature amplitude $X_L^{(sq)}(\vec{\rho})$. The squeezing has also a negative effect on the fidelity: the amplification (anti-squeezing) of the quadrature amplitude $P_L^{(sq)}(\vec{\rho})$, followed by scattering on the atomic density fluctuations. For a moderate squeezing, the relevant contribution to the noise covariance matrix is estimated [16] as $C^X(i, i) \sim \exp(2r)/n_a l \lambda$, where $\exp(r)$ is the amplitude squeezing and l is the parametric crystal length. For a sufficiently large atomic density this contribution is negligible.

Consider the contribution to the covariance matrix element $C^P(i, j) = \langle F_P^\dagger(i) F_P(j) \rangle$ coming from squeezed light:

$$C^{P(sq)}(i, j) = \langle X_L^{(sq)\dagger}(i) X_L^{(sq)}(j) \rangle =$$

$$\frac{1}{ST} \int_{S_i, S_j} d\vec{\rho}' d\vec{\rho}'' \int_T dt' dt'' \langle X_L^{(sq)\dagger}(\vec{\rho}', t') X_L^{(sq)}(\vec{\rho}'', t'') \rangle. \quad (13)$$

The covariance matrix $\langle X_L^{(sq)\dagger}(i) X_L^{(sq)}(j) \rangle$ of the squeezed light quadrature components averaged over the observation volume (the pixel area and the sampling time) determines the noise, the fidelity, the information capacity, etc. for optical schemes, considered earlier for optical images: the homodyne detection [17, 18], the quantum teleportation [9, 10] and the telecloning. In analogy to [10], we arrive at:

$$C^{P(sq)}(i, j) = \frac{1}{2} \int d\vec{q} B_\Delta(\vec{q}) \cos[\vec{q}(\vec{\rho}_i - \vec{\rho}_j)] G_X(\vec{q}, 0). \quad (14)$$

Here $G_X(\vec{q}, \Omega)$ is the Green function of the squeezed quadrature in the Fourier domain,

$$\begin{aligned} \langle X_L^\dagger(\vec{q}, \Omega) X_L(\vec{q}', \Omega') \rangle = \\ (2\pi)^3 \delta(\vec{q} - \vec{q}') \delta(\Omega - \Omega') \cdot \frac{1}{2} G_X(\vec{q}, \Omega), \end{aligned} \quad (15)$$

and $B_\Delta(\vec{q})$ is the delta-like even weight function, which originates from the integrals over the pixel surface.

Since the interaction time T is much longer than the coherence time of the squeezed light, only the low frequencies $\Omega \rightarrow 0$ contribute to (14). In terms of commonly used parameters of the wide-band squeezing, the Green function is

$$G_X(\vec{q}) = e^{2r(\vec{q}, \Omega)} \cos^2 \psi(\vec{q}, \Omega) + e^{-2r(\vec{q}, \Omega)} \sin^2 \psi(\vec{q}, \Omega). \quad (16)$$

Here $\exp[-r(\vec{q}, \Omega)]$ is the squeezing factor, and $\psi(\vec{q}, \Omega)$ is the orientation angle of the anti-squeezed axis of the uncertainty ellipse for a given frequency [17, 18].

For a single pixel the overall fidelity F_1 of the write-readout cycle of the quantum hologram is determined by the diagonal matrix elements: $C^X(i, i) = 0$, $C^P(i, i) = 1/2 + C^{P(sq)}(i, i)$ or $C^P(i, i) = C^{P(sq)}(i, i)$ for the coherent and the squeezed initial state of the atomic spin, respectively. As seen from (12), the ultimate value of fidelity $F_1 = 1$ is reached for zero diagonal elements of the noise covariance matrix. In Fig. 2 we plot the vari-

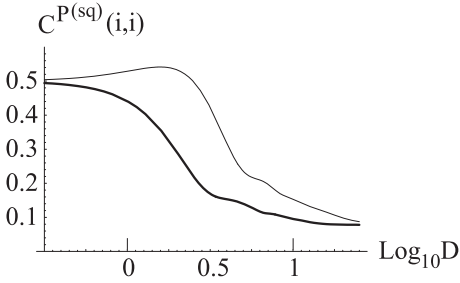


FIG. 2: Covariance matrix diagonal element for one pixel (the bold and hair lines – with and without phase correction of squeezing by means of a thin lens). Here $\psi(0, 0) = \pi/2$, $\exp[r(0, 0)] = 3$.

ance $C^{P(sq)}(i, i)$ for one pixel as a function of the pixel size $\Delta = \sqrt{S}$, normalized to the transverse coherence length l_d of the spatially multimode squeezed light. The latter scale is due to the diffraction of the downconversion light inside the nonlinear crystal when the propagation length is of the order of the length of parametric amplification. For a moderate squeezing a fair estimate for the coherence length is $l_d \sim \sqrt{l/2k_c}$ (here k_c is the downconversion wave vector inside the crystal). In our plots $D = \Delta/l_d$. A properly inserted thin lens is able to compensate the spatial frequency dispersion (rotation in the plane of quadrature components) of squeezing ellipses [17, 18]. The effect of compensation is also shown in our plots.

As shown in [10], the fidelity of the quantum state transfer for simple multipixel arrays scales approximately as the N -th power of the average fidelity per pixel, $F_{av} = (F_N)^{1/N}$. In order to find F_{av} for a large array, the covariance matrix is transformed to the diagonal form.

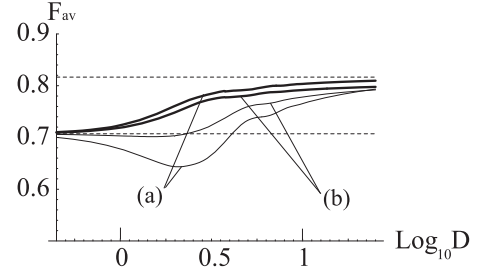


FIG. 3: Average fidelity per pixel for the initial coherent state (a) and the perfect squeezed state (b) of the collective atomic spin. The parameters of light squeezing are the same as in Fig. 2.

The eigenvectors of the matrix $\langle X_L^{(sq)\dagger}(i) X_L^{(sq)}(j) \rangle$ are given by the superpositions of amplitudes $X_L^{(sq)}$ with a quantized 2D “wave vector”.

The average fidelity per pixel for our model of quantum memory is plotted in Fig. 3. For the coherent initial state of the atoms (curves (a)), the upper limit $F_{av} = \sqrt{2/3} = 0.82$ can be reached for a large pixel size, $\sqrt{S} \gg l_d$, and perfect squeezing of light. The fidelity is limited by the vacuum fluctuations of the initial collective spin. For a small pixel, $\sqrt{S} \ll l_d$, the light squeezing has no effect. The lower limit $F_{av} = \sqrt{1/2} = 0.71$ corresponds to the vacuum noise of the initial state of both atoms and the light used for the readout of quantum memory. When both the collective atomic spin and the readout light are prepared in a perfect squeezed state (curves (b)), the perfect fidelity, $F_{av} = 1$, can be achieved for a large pixel size. The lower limit $F_{av} = \sqrt{2/3} = 0.82$ is due to the fact, that for a small pixel size the light fluctuations are restored back to the vacuum value. The quantum hologram hence provides the fidelity much higher than the best classical fidelity for the complete write plus readout protocol which according to [19] is 0.5.

To conclude, we have proposed an essentially parallel model of the quantum memory for light and analyzed its characteristic spatial scales, which in our scheme are associated with the transverse scales of the non-classical light used for the readout of the quantum hologram.

This research was supported by the RFBR – CNRS under Project 05-02-19646, by the Ministry of Science and Education of RF under Project RNP.2.1.1.362, by the INTAS under Project “Advanced Quantum Imaging and Quantum Information with Continuous Variables”, and by the EU projects QAP and COVAQIAL.

-
- [1] P. Zoller, T. Beth, B. Binosi, et al. European Physical Journal D 36 (2): 203-228, 2005
 - [2] A. Kuzmich and E. S. Polzik, chapter in the book: Quantum Information with Continuous Variables. Ed.

- S. Brainstein and A. Pati. Kluwer (2003).
- [3] J. Sherson, B. Julsgaard, and E. S. Polzik. *Advances in Atomic Molecular and Optical Physics* **54**, November (2006), Academic Press.
 - [4] Eisaman M.D., Andre A., Massou F., Fleischhauer M., Zibrov A.S., Lukin M.D. *Nature* **438**, 837-841 (2005).
 - [5] Chou C.W., Polyakov S.V., Kuzmich A., Kimble H.J.. *Phys. Rev. Lett.* **92**, 213601 (2004).
 - [6] Chaneliere T., Matsukevich D.N., Jenkins S.D., Lan S.Y., Kennedy T.A.B., Kuzmich A. *Nature* **438**, 833-836 (2005).
 - [7] B. Julsgaard, J. Sherson, J. Fiurasek, J. I. Cirac, and E. S. Polzik. *Nature* **432**, 482 (2004); quant-ph/0410072
 - [8] J. Sherson, H. Krauter, R. Olsson, B. Julsgaard, K. Hammerer, J. I. Cirac, and E. S. Polzik. *Nature* **443**, 557 (2006).
 - [9] I. V. Sokolov, M. I. Kolobov, A. Gatti, L. A. Lugiato. *Opt. Comm.* **193**, 175 (2001).
 - [10] A. Gatti, I. V. Sokolov, M. I. Kolobov and L. A. Lugiato. *Eur. Phys. J. D* **30**, 123 (2004).
 - [11] Yu. M. Golubev, T. Yu. Golubeva, M. I. Kolobov and I. V. Sokolov. *J. Mod. Opt.: Special issue on Quantum Imaging*, **53**, 699 (2006).
 - [12] K. Hammerer, K. Mølmer, E.S. Polzik, J.I. Cirac. *Phys.Rev. A.*, **70**, 044304 (2004).
 - [13] J. Sherson, J. Fiurášek, K. Mølmer, A. Sørensen, and E.S. Polzik. *Phys. Rev. A* **74**, 011802 (2006).
 - [14] A. Kuzmich, L. Mandel, and N. P. Bigelow, *Phys. Rev. Lett.* **85**, 1594 (2000).
 - [15] J.M. Geremia, John K. Stockton, Hideo Mabuchi, *Science* **304**, 270 (2004).
 - [16] D. V. Vasilyev, I. V. Sokolov, and E. S. Polzik, in preparation.
 - [17] M. I. Kolobov, I. V. Sokolov. *Sov. Phys. JETP* **69**, 1097 (1989)].
 - [18] M. I. Kolobov. *Rev. Mod. Phys.* **71**, 1539 (1999).
 - [19] K. Hammerer, M.M. Wolf, E.S. Polzik, J.I. Cirac, *Phys. Rev. Lett.* **94**, 150503 (2005).